JACC Vol. 30, No. 2
August 1997:436–43

Electrocardiogram-Gated Intravascular Ultrasound Image Acquisition After Coronary Stent Deployment Facilitates On-Line Three-Dimensional Reconstruction and Automated Lumen Quantification

CLEMENS VON BIRGELEN, MD,* GARY S. MINTZ, MD, FACC,† ANTONINO NICOSIA, MD, DAVID P. FOLEY, MB, MRCPI, PHD, WIM J. VAN DER GIESSEN, MD, PHD, NICO BRUINING, BSC, SERGEI G. AIRIIAN, MD, JOS R. T. C. ROELANDT, MD, PHD, FACC, PIM J. DE FEYTER, MD, PHD, FACC, PATRICK W. SERRUYS, MD, PHD, FACC

Rotterdam, The Netherlands and Washington, D.C.

Objectives. **This study evaluates the feasibility, reliability and reproducibility of electrocardiogram (ECG)-gated intravascular ultrasound (IVUS) image acquisition during automated transducer withdrawal and automated three-dimensional (3D) boundary detection for assessing on-line the result of coronary stenting.**

Background. **Systolic-diastolic image artifacts frequently limit the clinical applicability of such automated analysis systems.**

Methods. **In 30 patients, after successful angiography-guided implantation of 34 stents in 30 target lesions, we carried out IVUS examinations on-line with the use of ECG-gated automated 3D analyses and conventional manual analyses of two-dimensional images from continuous pullbacks. These on-line measurements were compared with off-line 3D reanalyses. The adequacy of stent deployment was determined by using ultrasound criteria for stent apposition, symmetry and expansion.**

Results. **Gated image acquisition was successfully performed in all patients to allow on-line 3D analysis within 8.7 ± 0.6 min (mean ± SD). Measurements by on-line and off-line 3D analyses correlated closely ($r \geq 0.95$), and the minimal stent lumen differed only minimally (8.6 ± 2.8 mm^2 vs. 8.5 ± 2.8 mm^2, $p = NS$). The conventional analysis significantly overestimated the minimal stent lumen (9.0 ± 2.7 mm^2, $p < 0.005$) in comparison with results of both 3D analyses. Fourteen stents (41%) failed to meet the criteria by both 3D analyses, all of these not reaching optimal expansion, but only 7 (21%) were detected by conventional analysis ($p < 0.02$). Intraobserver and interobserver comparison of stent lumen measurements by the automated approach revealed minimal differences (0.0 ± 0.2 mm^2 and 0.0 ± 0.3 mm^2) and excellent correlations ($r = 0.99$ and 0.98, respectively).**

Conclusions. **ECG-gated image acquisition after coronary stent deployment is feasible, permits on-line automated 3D reconstruction and analysis and provides reliable and reproducible measurements; these factors facilitate detection of the minimal lumen site.**

(J Am Coll Cardiol 1997;30:436–43)

Intravascular ultrasound (IVUS) permits detailed, high quality cross-sectional imaging of the coronary arteries in vivo. The normal coronary artery architecture, the major components of the atherosclerotic plaque and, in particular, changes that occur in coronary artery dimensions and anatomy during and after transcatheter therapy can be studied in vivo in a manner otherwise not possible (1–4). This includes direct visualization of intensely echoreflective (but radiolucent) stainless steel stent struts (5–11). In an attempt to reduce both the analysis time and the variability involved in planar IVUS measurements, automated three-dimensional (3D) image reconstruction and analysis systems have been developed (10–20). However, cyclic changes in coronary dimensions and the movement of the IVUS catheter relative to the coronary vessel wall frequently cause image artifacts (Fig. 1) that generally represent an important limitation to the applicability of 3D systems for quantitative analysis (17,21,22).

One method of limiting cyclic artifacts combines electrocardiogram (ECG)-gated image acquisition (22) and a previously validated program for automated 3D IVUS boundary detection (18,19). We applied this technique to the analysis of 34 coronary stents after successful angiography-guided implantation to determine the feasibility, reliability and reproducibility of this approach to assessing on-line procedural results.

From the Thoraxcenter, Division of Cardiology, University Hospital Rotterdam-Dijkzigt and Erasmus University, Rotterdam, The Netherlands; and †Washington Hospital Center, Washington, D.C. Dr. von Birgelen is the recipient of a fellowship of the German Research Society (DFG, Bonn, Germany).

Manuscript received December 10, 1996; revised manuscript received March 25, 1997, accepted April 16, 1997.

*Present address: Department of Cardiology, University Hospital Essen, Hufelandstrasse 55, 45122 Essen, Germany.

Address for correspondence: Patrick W. Serruys, Thoraxcenter, University Hospital Dijkzigt, P.O. Box 1738, 3000 DR Rotterdam, The Netherlands.

Published by Elsevier Science Inc.

0735-1097/97/$17.00
PII S0735-1097(97)00154-X

Abbreviations and Acronyms

CSA = cross-sectional area
ECG = electrocardiogram, electrocardiographic
IVUS = intravascular ultrasound
3D = three-dimensional
2D = two-dimensional

Methods

Study patients. The study was approved by the Medical Ethical Committee of the Erasmus University Hospital, Rotterdam. All patients provided written informed consent. The study group consisted of 30 patients (24 men, 6 women, mean age ± SD 59.1 ± 8.4 years) who had 34 stents implanted in 30 target lesions. To simplify the ECG-gated acquisition procedure, we chose for the study only patients who had 1) sinus rhythm, 2) ≤10 extrasystoles/min, and 3) no permanent or temporary pacemaker implantation.

Intervention procedures and coronary angiography. All patients received intravenous aspirin (250 mg) and heparin (10,000 U), and subsequent heparin was administered hourly to maintain an activated clotting time >300 s. The percutaneous transluminal angioplasty procedures were performed by using 8F femoral artery sheaths and 8F guiding catheters. All patients were undergoing elective stent implantation for stable (n = 14) or unstable (n = 16) angina; therefore, conservative balloon predilation was performed to enable stent placement but avoid unnecessary dissection. The stents were placed in the right (n = 20), left anterior descending (n = 9) and left circumflex (n = 5) coronary arteries. The following stents were used: Palmaz-Schatz stent (Johnson & Johnson Interventional Systems, n = 15); Wallstent (Schneider, Bulach, Switzerland, n = 11); Cordis balloon expandable coiled stent (Cordis Corporation, n = 4), Multilink stent (Advanced Cardiovascular Systems, n = 2); AVE Microstent (Applied Vascular Engineering, Edmonton, Alberta, Canada, n = 1); and NIR stent (Medinol, Ltd., Tel Aviv, Israel, n = 1). After the procedure, all patients were treated with an antiplatelet regimen of aspirin and ticlopidine.

On-line quantitative coronary angiography was performed with the CAAS II system (Pie Medical, Maastricht, The Netherlands) according to previously described methodology (10,11). The maximal diameter of the target segment and the interpolated reference diameter were used to select the diameter of the balloon-expandable stents. The interpolated reference diameter of the stented coronary segments ranged from 2.5 to 4.7 mm. The proximal and distal vessel diameter, interpolated reference diameter and lesion length were taken into account to select an appropriately sized self-expanding Wallstent (11). Adjunct balloon angioplasty was performed by using low compliance balloon catheters with a maximal nominal size of 3.74 ± 0.44 mm (balloon/preintervention reference = 1.24 ± 0.21; balloon/postintervention reference = 1.04 ± 0.14) at a maximal pressure of 16.4 ± 1.7 atm.

After IVUS imaging was performed, any further treatment was left to the discretion of the operator. Although additional IVUS examinations were not part of the protocol, and were, in fact, not performed, the operator was free to perform them, if he or she considered them necessary.

Angiographic end points. All procedures had achieved angiographic success before IVUS examinations were performed. A procedure was considered angiographically successful if all of the following three criteria were met: 1) smooth contour of the lumen silhouette in the stented segment, 2) diameter stenosis inside the stent in the "worst" (of at least two orthogonal) views <15% by quantitative on-line analysis, and 3) no inflow or outflow obstruction. IVUS examination was then performed.

IVUS imaging. IVUS imaging was performed after bolus injection of intracoronary nitroglycerin with use of a commercially available mechanical sector scanner (CardioVascular Imaging Systems) and 2.9F sheath-based IVUS catheters (MicroView, CardioVascular Imaging Systems). This catheter incorporates a 15-cm long sonolucent distal imaging sheath that alternatively houses the guide wire (during catheter introduction) or, after the guide wire has been pulled back, the 30-MHz beveled single-element transducer (during imaging).

First, a continuous motorized pullback of the IVUS transducer at a pullback speed of 0.5 mm/s (within the imaging sheath) was performed for conventional on-line two-dimensional (2D) cross-sectional IVUS analysis. Next, the transducer was readvanced for ECG-gated image acquisition. The basic settings of the IVUS machine remained unchanged to ensure an equal image quality during both pullbacks. Between both pullbacks there were no significant changes in the patients' heart rate and no differences in the occurrence of arrhythmias. The ECG-triggered pullback device uses a step-

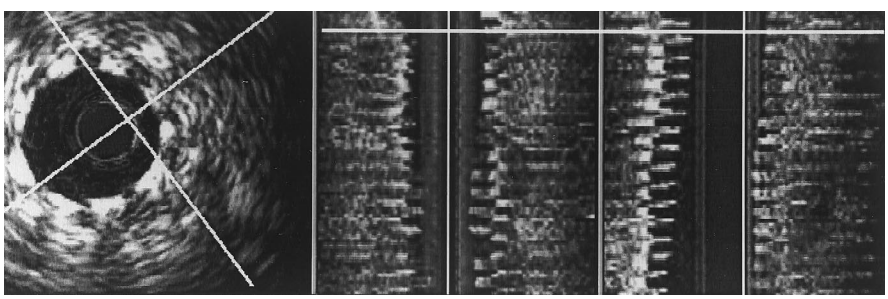

Figure 1. Cyclic artifact in 3D IVUS image set of stented coronary segment. **Center and right panels,** Saw-shaped artifacts in two perpendicular longitudinal sections after *non-gated* image acquisition, resulting from the cyclic movement of the echo-transducer relative to the coronary wall, may limit the on-line applicability of systems for automated contour detection. **Left panel,** Cross-sectional image corresponding to the horizontal cursor in the longitudinal sections.

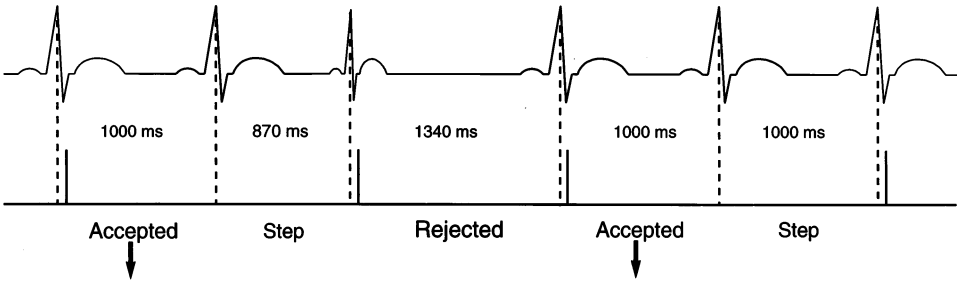

Figure 2. Principle of ECG-gated image acquisition and stepwise pullback. Images were acquired 40 ms after the peak of the R wave and only *accepted* for computer storage **(arrows)** if the time interval between two successive R waves met a predefined range. This range was based on data (mean RR interval ± 50 ms), taken before imaging was performed. If an RR interval was too long or short, images were *rejected*, and the transducer remained at this site until the image could be acquired during a heart cycle with an appropriate RR interval length. During the following heart cycle, the transducer was withdrawn 200 μm **(Step)** to the adjacent image acquisition site.

ping motor to withdraw the transducer in 0.2-mm axial increments through the stationary imaging sheath. The ECG-triggered pullback device is controlled by a 3D ultrasound work station (23) (EchoScan, TomTec, Munich, Germany). The work station receives a video input from the IVUS machine and an ECG signal from the patient. It measures the RR intervals over a 2-min period preceding the imaging sequence to define the upper and lower limits of acceptable RR intervals (mean value ± 50 ms). During the imaging sequence it considers heart rate variability and checks for the presence of extrasystoles. If the RR interval meets the preset range, images are 1) acquired 40 ms after the peak of the R wave, 2) digitized (by the work station), and 3) stored in the computer memory. After an image is acquired, the IVUS transducer is withdrawn 0.2 mm to acquire the next image at that site (Fig. 2).

IVUS analysis protocol. All 34 stented lesions were analyzed on-line by two experienced IVUS analysts who had no knowledge of each other's results. One analyst (called the "2D analyst") performed conventional manual tracing of the cross-sectional IVUS images. The second analyst (called the "3D analyst") analyzed the ECG-gated 3D IVUS images (18,19). The senior interventional cardiologists of the department decided that, to be clinically useful, all on-line analyses should be completed within ≤10 min.

After an interval of ≥4 weeks, the 3D analyst performed a blinded off-line reanalysis of the stored ECG-gated image set from all 34 stents. This off-line reanalysis had no time limit. Each image was carefully checked, the videotape was used to confirm the automated measurements, even small deviations were corrected, and the results were approved by two independent cardiologists, experienced in the use and analysis of IVUS imaging. The off-line reanalysis was performed within 28.7 ± 5.9 min and represented the maximal confidence measurements.

Intraobserver and interobserver variability of on-line 3D measurements of the stent cross-sectional area were determined from 10 randomly selected digitized stent image data sets (for a total of 1,112 cross-sectional IVUS images). Because actual on-line conditions cannot be reproduced, this comparison was obtained from simulated on-line conditions, especially a maximal analysis time of 10 min. Intraobserver variability was determined from repeated measurements performed by the 3D analyst; interobserver variability was determined by comparing the measurements of the 3D analyst and those of a third analyst who had no knowledge of previous data.

2D quantitative IVUS analysis. By using previously validated manual contour tracing techniques (24), the minimal lumen cross-sectional area (CSA) within the stented segment was measured and compared with the proximal and distal reference lumen CSA. These reference measurements were obtained from the most normal-looking cross-sections within 5 mm proximal and distal to the stent edges. In addition, the stent symmetry index (minimal/maximal stent diameter) was measured at the minimal lumen CSA site.

3D quantitative IVUS analysis. Quantitative 3D IVUS analysis was performed by using a contour detection program (Fig. 3) developed at the Thoraxcenter, Rotterdam. This system allows the automated analysis of up to 200 IVUS images. Two longitudinal sections are constructed in which contour detection is performed to identify regions of interest (center and range for boundary searching) on planar images. This procedure facilitates automated detection of the lumen boundary on the planar images with use of the minimum cost algorithm (18,19). The axial location of an individual planar image is indicated by a cursor that is used to scroll through the entire set of planar IVUS images to review the detected contours (Fig. 3). Corrections may be performed by "forcing" the contour through a visually identified point (minimum cost), which causes the entire data set to be updated (dynamic programming). This algorithm has been validated with use of a tubular phantom (18) and in histologic studies (19). Furthermore, the intraobserver and interobserver reproducibility of in vivo CSA measurements after nongated acquisition of IVUS images from nonstented atherosclerotic coronary arteries have been reported (18).

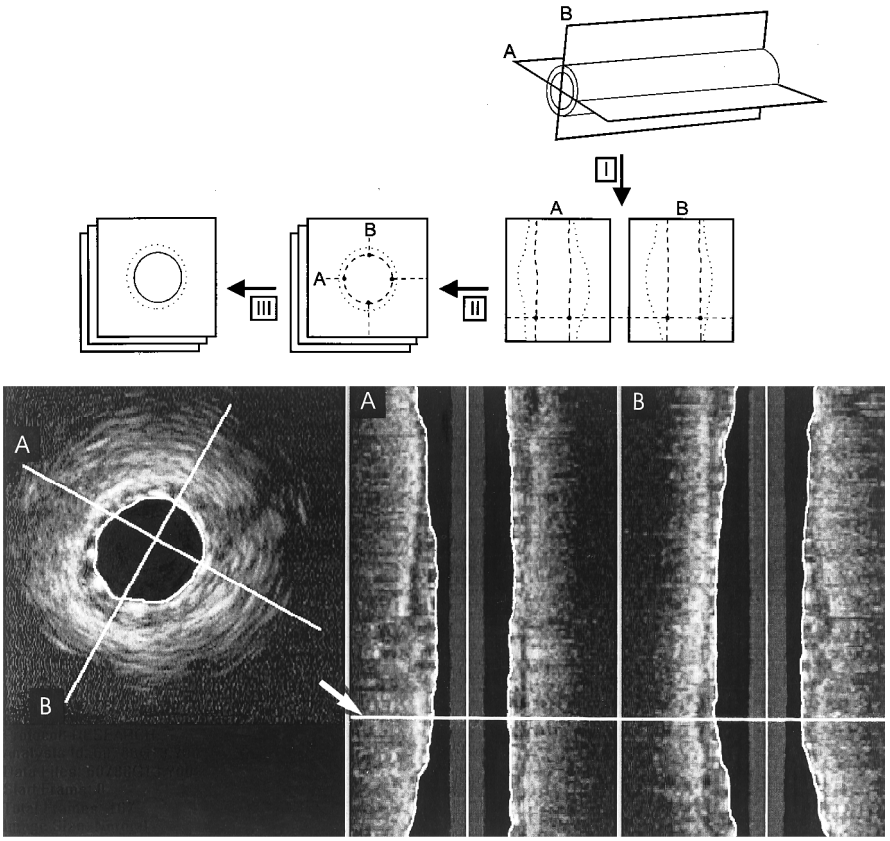

Figure 3. 3D quantitative IVUS analysis. **Upper panel,** Principle of automated lumen contour detection. Two perpendicular longitudinal sections (A, B) were reconstructed from image data of the entire 3D "stack" of images. The lumen contours were detected (I) by use of a minimum cost algorithm. Edge information of these longitudinal contours was represented as points on the planar images (II) and defined regions of interest (center and range of the boundary searching) that guided the final automated contour detection of the lumen boundary on the planar images. **Lower panel,** Clinical example of contour analysis in a stented coronary segment. A horizontal cursor **(arrow)** could be used to scroll through the entire set of planar images **(left).** This cursor indicated on the two perpendicular longitudinal sections (A, B) the site corresponding to the planar image displayed. On the longitudinal sections, note the relative smoothness of both lumen and external vascular boundaries.

Although the algorithm can also be used to detect the external vessel boundary (18,19), only the measurement of the lumen CSA (inside the echo-reflective struts of the metallic stents) and the stent symmetry ratio (i.e., minimal divided by maximal stent diameter) were used in the current study. Reference lumen CSA measurements were obtained at minimally diseased sites 5 mm proximal and distal to the stented segment.

IVUS criteria for optimal stent deployment. Three IVUS criteria, based on the experience of the Milan group (5,6) and our own data (11), were used to define optimal stent deployment: 1) apposition = complete stent apposition to vessel wall along the entire stented segment; 2) symmetry = ratio of minimal/maximal stent diameter (stent symmetry index) ≥0.7; 3) expansion = ratio of minimal stent CSA/mean reference lumen CSA ≥0.8; or, ratio of minimal stent CSA/distal reference lumen CSA ≥0.8 (if the site of the minimal stent CSA was in the distal third of the stent).

Statistical analysis. Quantitative data were given as mean value ± 1 SD; qualitative data were presented as frequencies. Continuous variables were compared by using a two-tailed Student *t* test and linear regression analysis; categoric variables were compared by the chi-square test or Fisher exact test. As proposed by Bland and Altman (25), the agreement of the different approaches was assessed by determining the mean value ± SD of the between-method differences. A p value < 0.05 was considered statistically significant.

Table 1. Comparison of On-Line and Off-Line Intravascular Ultrasound Analyses

	On-Line 2D	On-Line 3D	Off-Line 3D	Δ On-Line 2D vs. On-Line 3D	Δ On-Line 2D vs. Off-Line 3D	Δ On-Line 3D vs. Off-Line 3D
Stent						
Minimal lumen CSA (mm^2)	9.0 ± 2.7	8.6 ± 2.8	8.5 ± 2.8	0.4 ± 0.6*	0.4 ± 0.7†	0.1 ± 0.2
Symmetry index	0.83 ± 0.09	0.81 ± 0.07	0.81 ± 0.08	0.02 ± 0.07	0.02 ± 0.08	0 ± 0.02
Reference						
Proximal lumen CSA (mm^2)	12.7 ± 3.8	12.1 ± 3.8	12.4 ± 4.2	0.6 ± 2.3	0.3 ± 2.2	−0.3 ± 1.3
Distal lumen CSA (mm^2)	10.1 ± 2.8	10.1 ± 3.8	10.1 ± 3.7	0 ± 1.8	0 ± 2.1	0 ± 0.9
Suboptimal stent deployment	7 (21%)	14 (41%)	14 (41%)	−7 (−21%)‡	−7 (−21%)‡	0

*$p < 0.005$; †$p < 0.001$; ‡$p < 0.02$; all other differences were not significant. Values are expressed as mean value ± 1 SD or number (%) of stents. CSA = cross-sectional area; Δ = between-method difference; 3D, 2D = three- and two-dimensional intravascular ultrasound (IVUS) measurements, respectively.

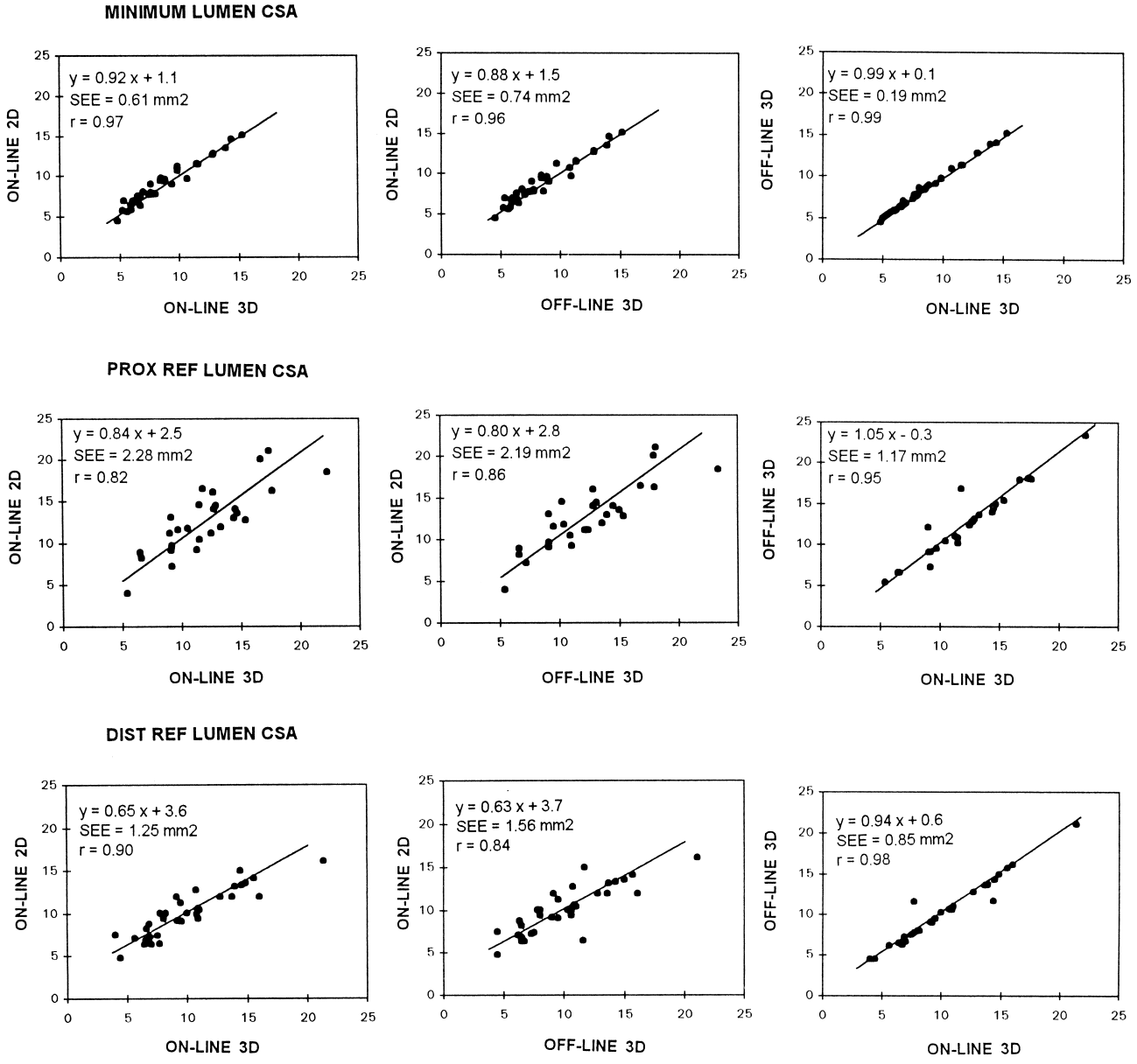

Figure 4. Results of linear regression analyses, comparing the lumen CSA measurements of the minimal stent **(upper panels),** proximal reference (PROX REF, **center panels**) and distal reference (DIST REF, **lower panels**), as obtained from on-line 2D and both on-line and off-line 3D IVUS analyses. Correlations were excellent, especially between on-line and off-line 3D IVUS measurements (the off-line 3D reanalysis represents the maximal confidence approach).

Results

Quantitative angiographic data. Before intervention, the minimal lumen diameter was 0.87 ± 0.42 mm, and the diameter stenosis 70.6 ± 13.7%. After stenting, a smooth angiographic lumen was achieved in all cases, with absence of inflow or outflow obstruction. The final minimal lumen diameter was 3.29 ± 0.41 mm with a corresponding diameter stenosis of 8.4 ± 3.4% (range 1% to 14%). According to the quantitative angiographic criteria, all stents were implanted successfully.

Feasibility of ECG-gated 3D IVUS image acquisition and analysis. After angiographically successful stent deployment, ECG-gated image acquisition was successfully performed in all patients with excellent tolerance. No subjective complaints of the patients were reported, and continuous ECG monitoring showed no evidence of ST segment alteration or increased frequency of arrhythmias during both gated and nongated IVUS imaging runs. The ECG-gated image acquisition required on average 4.6 ± 1.4 min (range 3.6 to 7.8), whereas the image acquisition during conventional continuous pullbacks required 1.7 ± 0.3 min (range 1.5 to 2.4, $p < 0.0001$). The on-line 3D analysis required 8.7 ± 0.6 min (range 7.3 to 10.0),

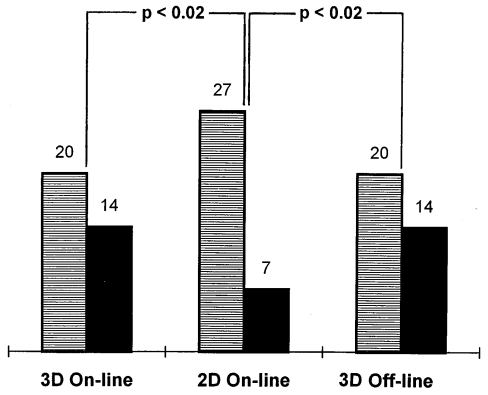

Figure 5. Detection of suboptimal stent deployment based on defined IVUS criteria. After angiography-guided stent implantation, off-line 3D analysis (providing the maximal confidence results) as well as on-line 3D analysis demonstrated that 14 stents (41%) failed to meet the IVUS criteria of optimal stent deployment, but only 7 (21%) of these stents were so classified by the on-line 2D analysis. **Striped bars** = IVUS criteria fulfilled; **solid bars** = IVUS criteria not fulfilled.

whereas reviewing the videotape and manually tracing the 2D IVUS images took 5.8 ± 0.7 min (range 4.8 to 7.4, $p < 0.001$).

IVUS measurements after stent deployment. The results of the different IVUS analyses are given in Table 1. There was a slight but significant overestimation of the minimal stent lumen CSA by the on-line 2D IVUS analysis when results were compared with those of both on-line and off-line 3D analyses ($p < 0.005$ and $p < 0.001$, respectively). The other variables measured (stent symmetry, proximal and distal reference lumen CSA) did not differ among analyses.

The between-method measurement variability, expressed as the standard deviation of the between-methods differences, was consistently higher for the on-line 2D measurement versus both the on-line and the off-line 3D measurements than for the two 3D measurements (Table 1). Nevertheless, the correlations among the CSA measurements obtained from the on-line 2D, on-line 3D and off-line 3D analyses were excellent (Fig. 4). Correlations of the stent symmetry measurements ranged from 0.62 (on-line 2D vs. 3D) to 0.98 (on-line 3D vs. off-line 3D).

IVUS criteria of optimal stent deployment. With the off-line 3D analysis (which provided the maximal confidence results), 14 (41%) of the 34 stents failed to meet the IVUS criteria of optimal stent deployment (Table 1). Only 7 of these stents were so classified by the on-line 2D analysis ($p < 0.02$), whereas all 14 stents were also identified by the on-line 3D analysis ($p < 0.02$ vs. on-line 2D analysis) (Fig. 5). Inadequate stent expansion was the constant reason for the failure to meet the deployment criteria ($n = 14$). There were no instances of incomplete stent apposition; the one case of stent asymmetry (which also had inadequate stent expansion) was revealed by both on-line 3D and off-line 3D analyses, but not by on-line 2D analysis.

Procedural outcome. After completion of the study protocol, any further treatment was left to the discretion of the operator. Additional angiography-guided balloon dilations were performed in six stents that had not met the criteria by both 2D and 3D IVUS ($n = 2$) or by 3D IVUS alone ($n = 4$). Lack of further stent expansion despite high pressure dilation with oversized balloons was the principal reason for omitting further balloon dilations. There were no procedural or post-procedural in-hospital complications.

Reproducibility of on-line 3D IVUS analysis. The intraobserver and interobserver differences of stent CSA measurements were 0.0 ± 0.2 mm^2 and 0.0 ± 0.3 mm^2 (relative SD 2.0% and 3.1%). The correlations were high (Fig. 6).

Discussion

IVUS insights into vessel and stent geometry (5–11) have played a central role in developing the concept of optimized stent deployment using adjunct high pressure balloon inflations (5,6,8,11,26). IVUS-guided stent implantation has reduced the incidence of stent thrombosis and permitted stenting without anticoagulation (5). These studies used planar IVUS analysis; however, changes of the stent dimensions observed during a transducer pullback are frequently smooth and gradual, and thus the minimal lumen area may be difficult to reliably identify visually. Automated 3D reconstruction and

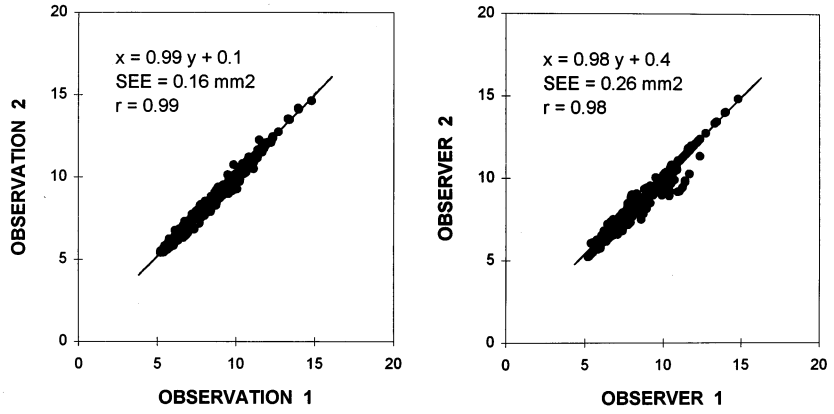

Figure 6. Intraobserver and interobserver measurement variability of on-line 3D IVUS. Correlation between the stent lumen CSA measurements (mm^2), provided by repeated analyses of the same observer (**left panel,** observations 1 and 2) and two independent observers (**right panel,** observers 1 and 2) using the 3D automated analysis method in ECG-gated IVUS image sets. Because actual on-line conditions cannot be reproduced, these data were obtained by using simulated on-line conditions, especially a maximal analysis time of 10 min.

analysis may therefore help to resolve this problem, but it must be both reliable and feasible during on-line application.

Previously, 3D reconstruction performed after stent implantation has been marred by cyclic image artifacts (18) (Fig. 1) that limited on-line application of automated 3D contour detection and analysis systems.

In the present study, to overcome this important limitation, we used ECG-gated IVUS image acquisition (23) and a validated automated 3D analysis system (18,19,27) on-line after angiography-guided stent deployment. The importance of ECG-gated image acquisition for off-line automated 3D IVUS measurements has been demonstrated by other groups (16,21) using alternative 3D contour detection systems. Sonka and colleagues (16) have stated that the correlation between observer-defined and automated lumen contours by their system improved as a result of ECG gating ($r = 0.91$ and 0.98 for nongated and ECG-gated, respectively) (16). We found that ECG-gated image acquisition resulted in much smoother vessel boundaries, readily facilitating the on-line contour detection process.

The main results of this study were that ECG-gated IVUS image acquisition and automated on-line 3D analysis 1) were feasible to evaluate the procedural results after stent deployment, 2) provided reliable and reproducible measurements of the lumen dimensions within the stented segment, and 3) facilitated the detection of the minimal lumen site. Despite the high correlation of the minimal lumen area measurements provided by the on-line 2D and 3D analyses, there was a significant overestimation of minimal lumen area with use of the 2D approach; this was confirmed by the off-line measurement. As a result, there were significant differences between the on-line 2D and 3D analyses in judging the adequacy of stent deployment by using the defined IVUS criteria. The high reliability of the on-line 3D approach in scrutinizing such criteria was confirmed by the off-line measurement. The on-line 3D analysis time (8.7 ± 0.6 min) of the present study is acceptably within the 10-min range set by the board of the Thoraxcenter senior interventional cardiologists. Nevertheless, in parallel with the advances in computer technology and further refinements in the software, further reduction of the analysis time can be expected.

Clinical implications. Although good clinical and angiographic results have been reported for coronary stenting without the use of IVUS (28,29), previous studies using conventional IVUS techniques (5,6,11) have suggested a considerable frequency of suboptimal results, a finding that is again confirmed by our methodology. We also found that conventional 2D IVUS itself underestimated the frequency of suboptimal stenting.

Numerous interventional cardiologists have praised IVUS as helpful in guiding (difficult) stent procedures and in investigating ambiguous angiographic results, but there is no blanket recommendation concerning the use of IVUS in routine stenting (26). However, the indication for stenting is currently broadening to smaller vessels, longer lesions, unfavorable morphology, multivessel disease and unstable syndromes, and the number of different types of stents available is increasing rapidly (30). Considering this increasing complexity of stenting procedures, a feasible and reliable IVUS analysis approach will remain at least extremely valuable, often necessary, and perhaps cost-effective, depending on long-term clinical results; this aspect will undoubtedly be an objective of future trials evaluating the usefulness of IVUS guidance in complex coronary stenting.

Study limitations. Nonuniform transducer rotation of mechanical IVUS catheters, noncoaxial catheter position or vascular curvatures may create image distortion and artifacts in both planar images and 3D reconstructions (17); however, segments are generally relatively straight after stenting. Although coronary angiography itself has several limitations, combined approaches using both angiographic and IVUS data for 3D reconstruction of the vessel may resolve many of the problems mentioned, but these techniques are laborious and still restricted to research (22). As 3D reconstructions of IVUS images generally do not depict the true spatial coronary geometry, careful interpretation by an experienced investigator is required.

Our experience suggests that ECG-gated image acquisition is feasible in 90% to 95% of patients referred for coronary intervention, but it may be difficult in patients with arrhythmias and even impossible in the presence of atrial fibrillation, unless cardiac pacing is performed. ECG-gated image acquisition (23) requires more time than conventional motorized pullbacks at a uniform speed; this longer duration may limit its use before interventions in patients with critical coronary stenoses. Further miniaturization of the IVUS catheters and the use of imaging wires (31,32) may soon help to overcome this limitation.

Conclusions. ECG-gated acquisition of IVUS images during automated transducer pullbacks is feasible after coronary stent deployment. The approach is clinically relevant, as it permits on-line automated 3D reconstruction and analysis, provides reliable and reproducible measurements of lumen dimensions and facilitates the detection of the minimal lumen area, thus guiding optimized stent deployment.

References

1. Fitzgerald PJ, St. Goar FG, Connolly AJ, et al. Intravascular ultrasound imaging of coronary arteries: is three layers the norm? Circulation 1992;86: 154–8.
2. Mintz GS, Painter JA, Pichard AD, et al. Atherosclerosis in angiographically "normal" coronary artery reference segments: an intravascular ultrasound study with clinical correlations. J Am Coll Cardiol 1995;25:1479–85.
3. Erbel R, Ge J, Bockisch A, et al. Value of intracoronary ultrasound and Doppler in the differentiation of angiographically normal coronary arteries: a prospective study in patients with angina pectoris. Eur Heart J 1996;17: 880–9.
4. Pinto FJ, St. Goar FG, Gao SZ, al. Immediate and one-year safety of intracoronary ultrasound imaging: evaluation with serial quantitative angiography. Circulation 1993;88:1709–14.
5. Colombo A, Hall P, Nakamura S, et al. Intravascular stenting without anticoagulation accomplished with intravascular ultrasound guidance. Circulation 1995;91:1676–88.
6. Goldberg SL, Colombo A, Nakamura S, Almagor Y, Maiello L, Tobis JM.

Benefit of intracoronary ultrasound in the deployment of Palmaz-Schatz stents. J Am Coll Cardiol 1994;24:996–1003.

7. Mudra H, Klauss V, Blasini R, et al. Ultrasound guidance of Palmaz-Schatz intracoronary stenting with a combined intravascular ultrasound balloon catheter. Circulation 1994;90:1252–61.
8. Görge G, Haude M, Ge J, et al. Intravascular ultrasound after low and high inflation pressure coronary artery stent implantation. J Am Coll Cardiol 1995;26:725–30.
9. Dussaillant GR, Mintz GS, Pichard AD, et al. Small stent size and intimal hyperplasia contribute to restenosis: a volumetric intravascular ultrasound analysis. J Am Coll Cardiol 1995;26:720–4.
10. von Birgelen C, Kutryk MJB, Gil R, et al. Quantification of the minimal luminal cross-sectional area after coronary stenting by two- and three-dimensional intravascular ultrasound versus edge detection and videodensitometry. Am J Cardiol 1996;78:520–5.
11. von Birgelen C, Gil R, Ruygrok P, et al. Optimized expansion of the Wallstent compared with the Palmaz-Schatz stent: online observations with two- and three-dimensional intracoronary ultrasound after angiographic guidance. Am Heart J 1996;131:1067–75.
12. Rosenfield K, Losordo DW, Ramaswamy K, et al. Three-dimensional reconstruction of human coronary and peripheral arteries from images recorded during two-dimensional intravascular ultrasound examination. Circulation 1991;84:1938–56.
13. Coy KM, Park JC, Fishbein MC, et al. In vitro validation of three-dimensional intravascular ultrasound for the evaluation of arterial injury after balloon angioplasty. J Am Coll Cardiol 1992;20:692–700.
14. Mintz GS, Pichard AD, Satler LF, Popma JJ, Kent KM, Leon MB. Three-dimensional intravascular ultrasonography: reconstruction of endovascular stents in vitro and in vivo. Clin Ultrasound 1993;21:609–15.
15. Matar FA, Mintz GS, Douek P, et al. Coronary artery lumen volume measurement using three-dimensional intravascular ultrasound: validation of a new technique. Cathet Cardiovasc Diagn 1994;33:214–20.
16. Sonka M, Liang W, Zhang X, De Jong S, Collins SM, McKay CR. Three-dimensional automated segmentation of coronary wall and plaque from intravascular ultrasound pullback sequences. In: Computers in Cardiology 1995. Los Alamitos (CA): IEEE Computer Society, 1995:637–40.
17. Roelandt JRTC, Di Mario C, Pandian NG, et al. Three-dimensional reconstruction of intracoronary ultrasound images: rationale, approaches, problems, and directions. Circulation 1994;90:1044–55.
18. von Birgelen C, Di Mario C, Li W, et al. Morphometric analysis in three-dimensional intracoronary ultrasound: an in-vitro and in-vivo study using a novel system for the contour detection of lumen and plaque. Am Heart J 1996;132:516–27.
19. von Birgelen C, van der Lugt A, Nicosia A, et al. Computerized assessment of coronary lumen and atherosclerotic plaque dimensions in three-dimensional intravascular ultrasound correlated with histomorphometry. Am J Cardiol 1996;78:1202–9.
20. Gil R, von Birgelen C, Prati F, Di Mario C, Ligthart J, Serruys PW. Usefulness of three-dimensional reconstruction for interpretation and quantitative analysis of intracoronary ultrasound during stent deployment. Am J Cardiol 1996;77:761–4.
21. Dhawale PJ, Wilson DL, Hodgson J McB. Optimal data acquisition for volumetric intracoronary ultrasound. Cathet Cardiovasc Diagn 1994;32:288–99.
22. von Birgelen C, Slager CJ, Di Mario C, de Feyter PJ, Serruys PW. Volumetric intracoronary ultrasound: a new maximum-confidence approach for the quantitative assessment of progression-regression of atherosclerosis? Atherosclerosis 1996;118 Suppl:S103–13.
23. Bruining N, von Birgelen C, Di Mario C, et al. Dynamic three-dimensional reconstruction of ICUS images based on an ECG-gated pull-back device. In: Computers in Cardiology 1995. Los Alamitos (CA): IEEE Computer Society, 1995:633–6.
24. Hodgson J McB, Graham SP, Savakus AD, et al. Clinical percutaneous imaging of coronary anatomy using an over-the-wire ultrasound catheter system. Int J Cardiac Imaging 1989;4:186–93.
25. Bland JM, Altman DG. Statistical methods for assessing agreement between two methods of clinical measurement. Lancet 1986;2:307–10.
26. Tobis JM, Colombo A. Do you need IVUS guidance for coronary stent deployment? Cathet Cardiovasc Diagn 1996;37:360–1.
27. Li W, von Birgelen C, Di Mario C, et al. Semi-automatic contour detection for volumetric quantification of intracoronary ultrasound. In: Computers in Cardiology 1994. Los Alamitos (CA): IEEE Computer Society; 1994:277–80.
28. Serruys PW, de Jaegere P, Kiemeneij F, et al., for the Benestent Study Group. A comparison of balloon expandable stent implantation with balloon angioplasty in patients with coronary artery disease. N Engl J Med 1994;331:489–95.
29. Fishman DL, Leon MB, Baim DS, et al., for the Stent REStenosis Study (STRESS) Investigators. A randomized comparison of coronary stent placement and balloon angioplasty in the treatment of coronary artery disease. N Engl J Med 1994;331:496–501.
30. Serruys PW, Kutryk MJB. The state of the stent: current practices, controversies, and future trends. Am J Cardiol 1996;78(Suppl 3A):4–7.
31. Di Mario C, Fitzgerald PJ, Colombo A. New developments in intracoronary ultrasound. In: Reiber JHC, van der Wall EE, editors. Cardiovascular Imaging. Dordrecht, The Netherlands: Kluwer Academic, 1996;257–75.
32. von Birgelen C, Mintz GS, de Feyter PJ, et al. Reconstruction and quantification with three-dimensional intracoronary ultrasound: an update on techniques, challenges, and future directions. Eur Heart J 1997;18:1056–67.